



Experimental evaluation of multi-antenna receivers for UAV communication in live LTE networks

Izydorczyk, Tomasz; Bucur, Madalina Cristina; Tavares, Fernando Menezes Leitão; Berardinelli, Gilberto; Mogensen, Preben Elgaard

Published in:
2018 IEEE Globecom Workshops (GC Wkshps)

DOI (link to publication from Publisher):
[10.1109/GLOCOMW.2018.8644068](https://doi.org/10.1109/GLOCOMW.2018.8644068)

Publication date:
2019

Document Version
Accepted author manuscript, peer reviewed version

[Link to publication from Aalborg University](#)

Citation for published version (APA):

Izydorczyk, T., Bucur, M. C., Tavares, F. M. L., Berardinelli, G., & Mogensen, P. E. (2019). Experimental evaluation of multi-antenna receivers for UAV communication in live LTE networks. In *2018 IEEE Globecom Workshops (GC Wkshps)* Article 8644068 IEEE (Institute of Electrical and Electronics Engineers). <https://doi.org/10.1109/GLOCOMW.2018.8644068>

General rights

Copyright and moral rights for the publications made accessible in the public portal are retained by the authors and/or other copyright owners and it is a condition of accessing publications that users recognise and abide by the legal requirements associated with these rights.

- Users may download and print one copy of any publication from the public portal for the purpose of private study or research.
- You may not further distribute the material or use it for any profit-making activity or commercial gain
- You may freely distribute the URL identifying the publication in the public portal -

Take down policy

If you believe that this document breaches copyright please contact us at vbn@aub.aau.dk providing details, and we will remove access to the work immediately and investigate your claim.

Experimental evaluation of multi-antenna receivers for UAV communication in live LTE networks

Tomasz Izydorczyk^{*}, Mădălina Bucur^{*}, Fernando M. L. Tavares^{*}, Gilberto Berardinelli^{*} and Preben Mogensen^{*†}

^{*}Department of Electronic Systems, Aalborg University (AAU), Denmark

[†]Nokia Bell Labs, Aalborg, Denmark

E-mail: {ti, mcb, ft, gb, pm}@es.aau.dk

Abstract—Unmanned Aerial Vehicle (UAV) communication is known to suffer from significant interference due to the clearance of the radio paths with ground base stations. Multi-antenna receive combining has the promise of alleviating the impact of interference, translating to improved connectivity performance. In this paper, we evaluate the performance of Conventional Beamforming (CB) and Maximum Ratio Combining (MRC) receivers for UAV communication based on live Long Term Evolution (LTE) networks. Our measurement setup consists of nine Universal Software Radio Peripheral (USRP) boards and a circular antenna array with sixteen elements. The LTE signals are recorded at different UAV flight heights in urban environments, and processed offline. Results show similar Signal-to-Interference-plus-Noise Ratio (SINR) performance by MRC and CB, with CB slightly outperforming MRC provided knowledge of LTE signal structure is used for the beam selection. No significant dependency from the flight height has been observed. The outage probability analysis further emphasizes the benefits of using CB in the studied scenarios.

I. INTRODUCTION

The use of Unmanned Aerial Vehicles (UAV), commonly referred to as drones, is expected to grow rapidly in the next few years, fueled by multiple new use cases. In [1], the authors indicate different data traffic patterns which characterize UAV-ground communication links. Many surveillance applications will require extra uplink capacity to transmit video feeds from cameras installed on a UAV [2]. On the other hand, ground-to-UAV communication, traditionally referred as downlink, will be largely dominated by Communication and Control (C2) messages, which can be characterized as a low-throughput messages containing commands for UAV flight path alternation.

Cellular networks such as Long Term Evolution (LTE) are considered a promising solution for future UAV communication, due to their widespread coverage and instantaneous availability. The potential of LTE in the context of UAV communication was recognized by the Third Generation Partnership Project (3GPP) and a study item [3] was created. However, cellular networks are optimized for terrestrial communications. Relevant parameters such as antenna down-tilt or power control settings are set with the aim of maximizing the performance of ground-level communications.

Since it is not provisioned to change cell-wide settings, research activity focused on assessing the quality of UAV communication over existing cellular networks. In [4] and [5],

the radio channel characterization based on experimental measurement campaigns was studied with particular focus on path loss modeling. It has been observed that at sufficiently high UAV flight altitudes, the propagation becomes more similar to free-space. This is due to the more probable Line-of-Sight (LOS) link between Base Station (BS) and the UAV. However, as shown in [6], the Signal-to-Interference-plus-Noise Ratio (SINR) observed by UAVs is significantly lower in comparison to the terrestrial User Equipment (UE) given the LOS conditions on the vast majority of interfering links. This problem was further addressed in [7] and [8] where analytical models for interference and coverage were developed.

Multiple research activities have focused on interference mitigation schemes for UAVs. Physical layer techniques, such as beamforming and multi-antenna received signal combining, are expected to improve the SINR levels experienced by UAVs. In [9], the authors show promising simulation results of interference mitigation using different multi-antenna techniques including narrow beam antenna selection and Interference Rejection Combining (IRC).

As multiple analytical attempts to quantify and combat the interference impact were made, only a few experimental studies were performed. Studies based on real network measurements can help mitigate the simulation bias and assess the problem in real propagation conditions. Very often they allow to detect previously unforeseen problems and effects overlooked in simulation assumptions. In [10], authors discuss the impact of non-ideal antenna pattern and time-variant UAV orientation on UAV connectivity using IEEE 802.11 network. In [11], authors experimentally quantify the uplink interference introduced to the network by the UAV. Based on the input from the network operator, they estimate the interference caused by their UAVs constantly transmitting the uplink data to the network. Those interference levels were later used in [12] to simulate the performance of interference cancellation schemes using an ideal IRC receiver.

Even though these studies showed the potential of the multi-antenna techniques, the methodology used within cannot fully reflect their performance in a real network. In the existing literature, the experimental input is indeed limited to the interference power levels, and receiver performance is still evaluated by assuming ideal knowledge of the radio channel responses of the received signals. This may severely bias the

estimated outcome of the studied receivers. A workaround to this problem is to test the multi-antenna techniques directly on recorded live network signals to quantify their actual benefits.

In this work, we experimentally evaluate the performance of multi-antenna techniques at UAV flight heights, based on live Long Term Evolution (LTE) cellular signals. In view of recorded I/Q samples from live cellular networks, the link performance of Maximum Ratio Combining (MRC) and Conventional Beamforming (CB) techniques is compared with single antenna UAV links. By using Universal Software Radio Peripheral (USRP)-based setup and offline signal processing, we measure the average SINR of different LTE control channels and use it as a metric to compare single antenna links to MRC and CB using multiple beam selection strategies. Further, we also study the performance in low-SINR regime, by discussing the applicability of multi-antenna techniques for ensuring uninterrupted connectivity.

The rest of the paper has the following structure. In Section II the measurement methodology is described. This is followed by the description of the post-processing method in Section III. Section IV-A discusses the levels of interference experienced at the UAV. This section is followed by Section IV-B, where the performance of multi-antenna techniques is studied. The work is concluded with Section V.

II. MEASUREMENT METHODOLOGY

A. Hardware setup

The measurement setup consists of a sixteen-antennas uniform circular array, which is connected with eight fully synchronized and calibrated USRP boards. Each of the boards is equipped with two receiver (RX) chains. The boards are then connected to a PXI-8820 controller using a PXIe-1085 chassis which acts as a data hub. On Figure 1, the block diagram of the setup is presented. The main advantage of using USRPs and the PXI controller is the possibility to record a large amount of data without any real-time processing. UAV-based setups are usually power-limited and due to payload limitations their usage is reduced to the simple scanner-like measurements. By using our setup, measured samples can later be used as input in a wide range of activities ranging from channel propagation studies to advanced transceiver design.

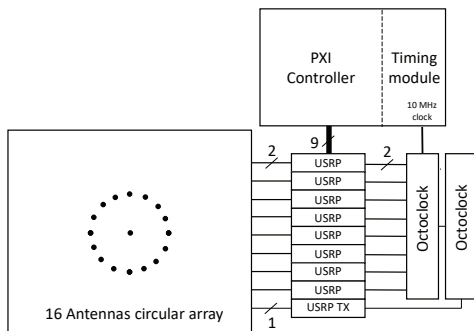


Fig. 1. Measurement setup schematic

1) *Antenna array*: Sixteen monopole antennas disposed in an uniform circular array were manufactured to record signals from the downlink (DL) part of LTE Band 3 used by two Danish network operators (center frequencies of 1.815 GHz and 1.87 GHz). They are installed on an aluminum ground plane and are connected to the USRP boards using three-meter-long RG233 cables.

Although it is highly unlikely that first autonomous UAVs will be equipped with many antennas, by using this amount one can set the focus on the comparison among different receiver techniques in their upper-bound performance limits. It is worth mentioning that due to raw signal recordings, in Section IV-B the performance of MRC with reduced number of antennas is also studied by simply discarding the data recorded by some of the antennas.

2) *USRP and PXI controller*: Eight USRP 2953R boards are used to record the LTE DL Band 3 signals at 40 MS/s. They perform digital down conversion and stream the I/Q samples via fast Peripheral Component Interconnect (PCI) bus to the PXI controller. To ensure the perfect time/frequency alignment among the eight boards, the external 10 MHz clock is generated by the timing module NI PXIe-6674T and redistributed to all boards by two Octoclocks CDA-2990.

Since digital beamforming algorithms require alignment in both frequency and phase, a calibration procedure for the receiving USRPs is required. Another USRP board is used for transmission of a single-tone out-of-band signal from the antenna placed at the center of the array. Given the omnidirectional radiation pattern, all sixteen antennas receive the calibration tone at the same time and with the same phase. By using one of the antennas as a reference, the random phase offset of each USRP can be compensated.

3) *Assembled setup*: The described setup was assembled in a metal structure and was safely lifted using a crane as presented in Figure 2. The antenna array was attached to the structure and covered by a hemisphere radome to prevent any short-circuit in case of rain. The radome was tested to be transparent for the radio waves at the measured frequency.

B. Measurement campaign

Seven different locations in Aalborg, Denmark were selected for the measurements: three in the city center (surrounded by tall buildings with average height 20 m and multiple BS), one in the suburbs (surrounded by houses and limited number of BS), one in a rural area (with limited coverage and interference levels) while the remaining two in the industrial part of the city. Combined altogether, they provide a set of diverse propagation environments observed by flying UAV.

In each location, the designed setup was lifted using the crane up to a 40 m height. Starting from the ground, 100 ms snapshots of LTE signals were taken every 5 m. On average, eight snapshots were recorded for each of the two network operators at each height. To avoid the possible signal blockage due to the existence of the metal cage and the ground plane, half of the measurements were taken with the antenna array pointing downwards (as can be seen at the right side of

Figure 2) while another half with the array pointing upwards. There were on average 156 snapshots taken per location.



Fig. 2. Assembled setup lifted to 40 meters high by a crane (left) and zoomed (right)

III. POST-PROCESSING

The performance of CB and MRC is studied in the post-processing. The case of a UAV equipped with a single antenna receiver processing is also included as a benchmark. Other techniques, such as IRC and advanced beamforming (with for example multiple beams or null-steering), are left for future work. The total number of 1069 snapshots are independently processed as presented in Figure 3. The signal received by each antenna is phase shifted to compensate for the random phase offset introduced by each USRP board. Further processing depends on the receiver technique and is described in the next subsections.

The following notation is used. The received and phase-calibrated N_{RX} input data streams are collected in a matrix \mathbf{S} of size $[N_{RX} \times N_{samp}]$, where $N_{samp} = 4 \cdot 10^6$ corresponds to the number of recorded samples. \mathbf{y}_i is the resulting vector of size $[1 \times N_{samp}]$ after beamforming operation on signal \mathbf{S} and r is the single complex number after equalization of various LTE physical channels.

A. Single-antenna receiver

After phase calibration, only the first row ($N_{RX} = 1$) of the recorded data matrix \mathbf{S} is processed by the LTE receiver which is designed based on the Matlab LTE toolbox. The reception methodology follows the procedure implemented in a typical LTE UE. First, the received signal is downsampled to 1.92 MHz and synchronization to the network is performed based on the LTE Primary and Secondary Synchronization Signals (PSS and SSS). The correlation between all 504 Physical Cell Identities (PCIs) and received signal is computed. After frame offset correction, attachment is made to the cell with the strongest power at the output of the correlator.

In the next step, after synchronization and coarse channel estimation based on the synchronization signals, Physical Broadcast Channel (PBCH) containing Master Information Block (MIB) is equalized using a matched filter. After MIB decoding information on the bandwidth of the LTE signal is retrieved. This information is used to resample the signal to the sampling

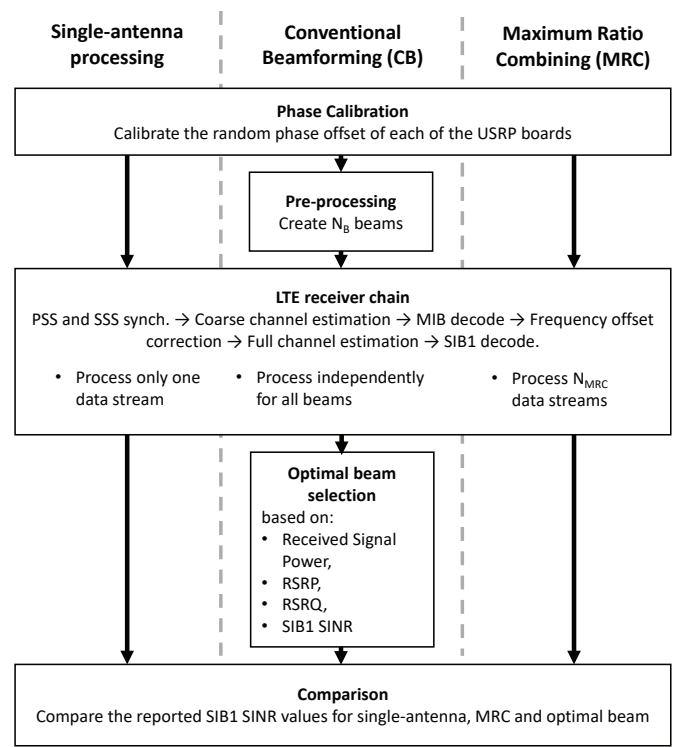


Fig. 3. Post-processing flow chart

rate matching the given bandwidth. Later, the frequency offset is estimated and corrected, which is followed by the estimation of the channel matrix over the entire operational bandwidth based on the Cell-specific Reference Signals (CRS). From the estimated channel matrix the Reference Signal Received Power (RSRP) and the Reference Signal Received Quality (RSRQ) are computed following the 3GPP specifications [13].

Finally, provided sufficient signal quality, the LTE receiver attempts to decode the System Information Block 1 (SIB1) using as before a matched filter for the detection of Physical Downlink Shared Channel (PDSCH). If successful, the Error Vector Magnitude (EVM) and SINR of this control channel are computed. Due to the length of the recorded snapshot, there are on average five instances of SIB1 message in each of them. The computed SINR values are averaged and a single value per snapshot is reported. Due to the averaging and different SIB1 locations in the time-frequency grid among different cells, the effect of the different cell loads of the network can be captured.

B. Conventional beamforming receiver

To evaluate the performance of beamforming, in pre-processing, $N_b = \{16, 360\}$ beams pointing towards different azimuth and elevation angles are created and the received signal impinging the array is weighted by each of these beams. The resulting signals \mathbf{y}_i are independently decoded at the receiver for each created beam $i \leq N_b$. Later, after the receiving process is done for all of the beams, the optimal one is selected, while others are discarded. CB is used to create a beam with the half-power beamwidth equal to 22.5° .

The received and phase-calibrated input data streams \mathbf{S} are weighted as below:

$$\mathbf{y}_i = \left(e^{-2\pi j \frac{r}{\lambda} \cos(\varphi_i) \cos(\theta_i - \theta)} \right)^H \cdot \mathbf{S} \quad (1)$$

where θ_i and φ_i refer to the azimuth and elevation angle for a given beam i , r is the radius of the antenna array equal 20 cm, λ is the wavelength equal to 0.1652 m or 0.1603 m for two network operators and θ is the antenna position-dependent column vector of angles of size $[N_{RX} \times 1]$. $(\cdot)^H$ denotes the hermitian operator.

After beamforming, all the \mathbf{y}_i beams are processed identically by the LTE receiver as a single-antenna stream. The next step is to decide which of the created beams should be used by the receiver for further processing of the data channels. The so-called *optimal beam* is the beam which maximizes the UE performance quantified by one of the various metrics. Given the near real-time requirements and UAV power constraints, the following metrics for selecting the optimal beam, varying with receiver complexity are investigated:

- **Received signal power:** This is the simplest and least computationally-heavy metric proposed. The receiver computes the power level M_i of the beamsteered input signal before the LTE receiver for each of the beams i , based on the given formula:
$$M_i = 10 \cdot \log_{10} (|\mathbf{y}_i|^2) \quad (2)$$
- **RSRP:** After the channel estimation for all of the beams, their respective RSRP is computed. Since this metric is constantly measured by the ground-level UE to assess the quality of the signal from the attached and neighbor cells (for the handover procedure), its use does not require any additional processing. The metric can be written as: $M_i = RSRP_i$.
- **RSRQ:** The optimal beam is the beam which maximizes the RSRQ metric. The difference between using RSRP and RSRQ metrics lies in the fact that RSRQ accounts for the existence of interference while RSRP does not. The metric is therefore: $M_i = RSRQ_i$.
- **SIB1 SINR:** This is the most computationally-heavy method requiring long LTE Receiver processing to estimate the SIB1 SINR: $M_i = SINR_i$.

The optimal beam B_{opt} is the beam which maximizes the given metric as below:

$$B_{opt} = \underset{i=1:N_b}{\operatorname{argmax}} M_i \quad (3)$$

After selection of the optimal beam, processing is ultimated and other beams are discarded.

C. MRC receiver

After phase calibration, a subset of signals received from N_{MRC} antennas (with $2 \leq N_{MRC} \leq 16$) is processed. Upon time and frequency offsets estimation, the receive combining is performed as follows:

$$r = (\mathbf{h}^H \mathbf{h})^{-1} \mathbf{h}^H \mathbf{x} \quad (4)$$

where \mathbf{x} denotes the $[N_{MRC} \times 1]$ vector of a received resource element over the N_{MRC} antennas, \mathbf{h} is the corresponding estimated channel vector, and r is the resultant estimated data symbol. Note that (4) is applied for both MIB and SIB detection. The remaining operations follow the steps of the single antenna receive processing.

IV. PERFORMANCE ANALYSIS

A. Single antenna performance from a UAV's perspective

Before the evaluation of multi-antenna techniques, the performance of a single antenna receiver is analyzed to show the signal degradation experienced by the UAV as it takes off to the air. The analysis is performed over all the recorded snapshots.

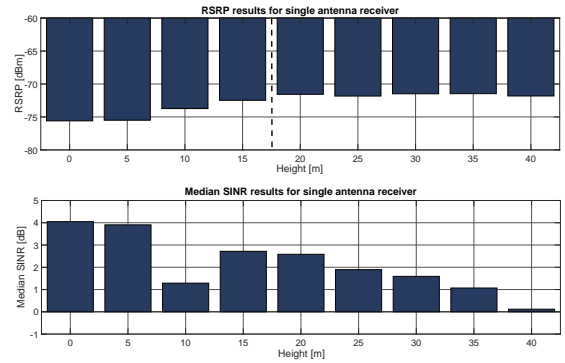


Fig. 4. Median RSRP and SINR values of a single antenna receiver against height

Figure 4 depicts the reported median RSRP and SINR values considering all the recorded locations for the single antenna receiver. As expected, as the height increases, the received signal becomes strongly affected by interference resulting in a SINR drop from 4 dB at the ground level up to 0 dB at 40 m. The sudden SINR drop was observed at about 10 m. This may be due to the UAV leaving the BS's main beam, which is pointed downwards towards the ground. At higher heights, with increased radio clearance, this issue is mitigated by reception of signal from a different BS.

RSRP results allow to notice a distinct behavior. It can be observed that there is a separation of the results, based on height. From ground level to approximately 15 m, the RSRP values vary and increase with height from -76 to -72 dBm. After reaching 20 m - the average height of buildings in Aalborg, the reported RSRP stabilizes at around -72 dBm. This behavior was used to split the recorded snapshots into two groups, indicated by the dashed line on the figure: *take-off zone* with limited interference (0 - 15 m) and *low flight level zone* with increased interference levels (20 - 40 m).

B. Performance evaluation of multi-antenna receivers

All the results presented next are based on measurements collected from all locations for the aforementioned sets of heights. There was no significant difference in the observed receiver performance depending on the recorded location.

Implicitly, the same data set was used for all the receiver types considered in this paper. The usage of SINR gains as a metric for the comparison is therefore feasible.

1) *MRC with 2, 4, 8 and 16 antennas array*: First, the gain of the MRC considering the different number of antenna elements with respect to the single antenna case is analyzed. As already mentioned, the processing is performed over subsets of the received signals.

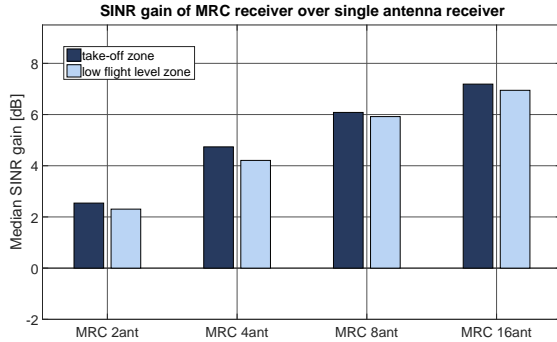


Fig. 5. Comparison of median SINR gains of MRC over a single antenna receiver

Figure 5 shows a clear improvement in the receiver's performance as the number of elements is increased. In the take-off zone, by adding only a second antenna a gain of 2.5 dB is observed, while the sixteen-antennas array provides a gain of 7.1 dB. However by adding more antenna elements, the additional gain decreases rapidly to only 1.1 dB. The observed array gains are also significantly lower with respect to the theoretical ones computed as $G_{array} = 10 \cdot \log_{10}(N_{RX})$. As an example, theoretical array gain G for $N_{RX} = 16$ number of elements is 12 dB and is 4.9 dB higher than the measured one. Both phenomena are the result of the observed interference on the CRS which affects the quality of the channel estimation. With an increased number of received antennas, the estimation error becomes more significant resulting in a lower-than-expected gain. It is expected that by replacing the least square channel estimator with a more advanced method, the performance gain can be slightly improved.

Very little difference was noted while comparing the SINR gains for the take-off and low level flight zones. Even with increased interference levels at the higher heights, the overall performance drop of MRC was comparable with the respective performance drop of a single antenna receiver resulting in a comparable gain. In the worst case, for the four-antenna receiver a drop of 0.5 dB was observed.

2) *Conventional beamforming*: Second study considered the performance gains of using the CB for UAV communications. The simple strategy, where $N_b = 360$ beams are uniformly spaced only in the azimuth plane assuming $\varphi = 0^\circ$ elevation angle was studied. Figure 6 shows the obtained performance gains with respect to a single antenna receiver, considering the beam selection criteria as described in Section III-B. The gain of MRC with sixteen antennas was

added as a reference. In an upper-bound case of a beam-selector using an optimal SINR method, gains of 9.46 dB over a single antenna receiver and 2.52 dB over MRC were observed.

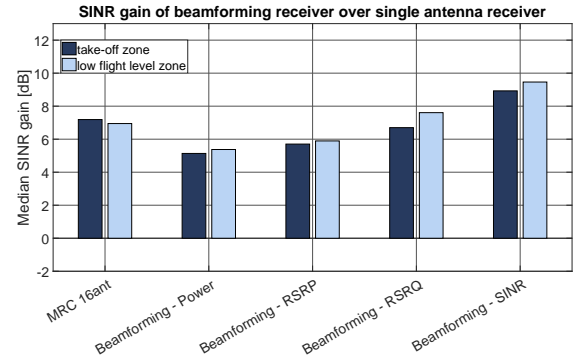


Fig. 6. Comparison of beamforming gains over a single antenna receiver

Surprising results were observed by looking at the performance of different beam-selectors. Using the received signal power as selection criterion provides the smallest gain among the considered cases. This gain is relatively similar to the one using RSRP as a beam selector, even though the latter exploits the structure of the LTE signal. Only if metrics with knowledge of interference are exploited (RSRQ or SINR), the observable gains are higher than the MRC ones. Lastly, it can be observed that the performance gains are higher for low flight level zone than the gains that can be attained at the take-off zone. CB technique appears to benefit in scenarios where the LOS path exists regardless of increased interference levels.

Other beam steering strategies were also considered. A performance gain of less than 0.1 dB was observed if beamforming was done considering different elevation angles φ (at a below 1° resolution). An average performance drop of approximately 12% was observed if the number of possible beams N_b was reduced to sixteen, although the similar trends between different selectors as on Figure 6 were observed. This was expected as the subspace covered by the beams was reduced. However, it can be argued that the performance loss is negligible comparing with the reduced complexity of the beamformer.

From a receiver perspective, the reported values for RSRP and RSRQ are already available and their use as beam selection criteria is straightforward. Even better performance can be achieved by using SIB1 SINR reported values, but this information is not as easily accessible to the receiver, as are the RSRP and RSRQ measurements. It requires the receiver to perform decoding of additional physical channels to attain it, which requires considerable processing time.

To complement this study, Figure 7 presents how the optimal elevation angle changes with the height. As expected, in the take-off zone the optimal elevation angles are significantly higher than above the rooftops where signals are usually coming with low elevation angle. These findings can potentially

justify the beam-steering only within an azimuth plane, thus reducing receiver complexity.

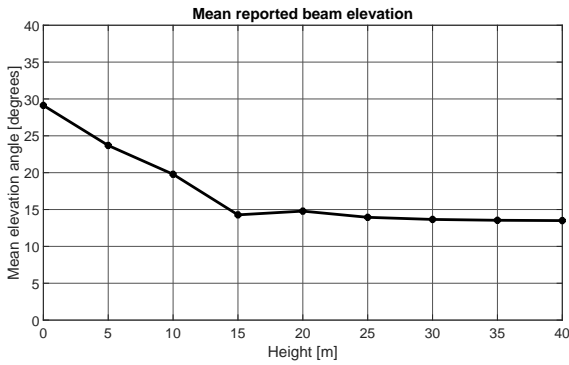


Fig. 7. Measured optimal elevation angle

3) *Outage comparison*: One of the most important aspects of UAV connectivity is its reliability. In case of very low SINR, there may be no connection between BS and UAV, referred later as an *outage*, which can result in a life-threatening accident. In this work, a snapshot is defined to be in outage, if none of the SIB1 messages was decoded correctly. Implicitly, outage also occurs in all cases when MIB decoding failed.

In all previous studies, snapshots detected to be in outage were assigned a fixed low SINR value, such that their effect was captured in the median calculation. Figure 8 presents the percentage of snapshots being in outage regardless of the measured height. The 6.4% (68 out of 1069) of snapshots processed using a single antenna were not decoded correctly. By using any of the multi-antenna techniques, this value can be greatly decreased. Surprisingly, beamforming techniques can help to further reduce the outage percentage compared to MRC. As beamforming is being done before any LTE processing, by co-phasing the received signal, the robustness of PSS/SSS synchronization is improved and number of outages further reduced. There were no outages reported for CB case with SINR used as a beam selector. This indicates that for all snapshots, there is at minimum one beam ensuring network connectivity and the observed outage is not related to limited received signal strength.

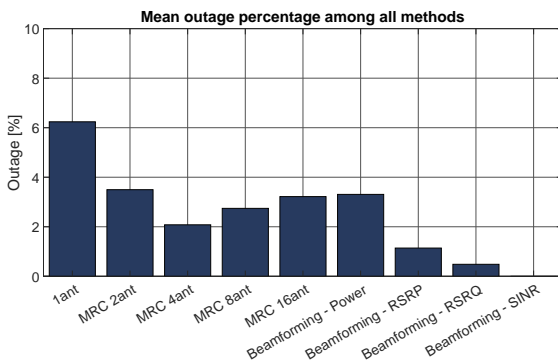


Fig. 8. Percentage of outage calculated for all methods

V. CONCLUSIONS

In this work, the performance of multi-antenna receiver techniques for UAV communications was studied. Due to the interference resulting in imperfect channel estimation, the observed gains of MRC were lower than theoretical and saturated with increased number of antennas. Beamforming methods are promising alternatives to the MRC. They outperform MRC if LTE channel knowledge is exploited and provide similar gain also when a limited number of beams is considered. Surprisingly, height dependency has a very little impact on the observed performance, with similar results observed at both take-off and low height flying zones. It is expected that the observed changes can become more significant at an increased flight height.

ACKNOWLEDGMENT

This work has been supported by the cooperative project VIRTUOSO, partially funded by Innovationsfonden Denmark.

REFERENCES

- [1] S. Hayat, E. Yanmaz, and R. Muzaffar, "Survey on unmanned aerial vehicle networks for civil applications: A communications viewpoint," *IEEE Communications Surveys Tutorials*, vol. 18, no. 4, pp. 2624–2661, 2016.
- [2] S. Qazi, A. S. Siddiqui, and A. I. Wagan, "UAV based real time video surveillance over 4G LTE," in *2015 International Conference on Open Source Systems Technologies (ICOSST)*, pp. 141–145, Dec 2015.
- [3] "Study on enhanced LTE support for aerial vehicles (release 15)," Tech. Rep. TR 36.777 V0.4.0, 3GPP, November 2017.
- [4] A. Al-Hourani and K. Gomez, "Modeling cellular-to-UAV path-loss for suburban environments," *IEEE Wireless Communications Letters*, vol. 7, pp. 82–85, Feb 2018.
- [5] R. Amorim, H. Nguyen, P. Mogensen, I. Z. Kovács, J. Wigard, and T. B. Sørensen, "Radio channel modeling for UAV communication over cellular networks," *IEEE Wireless Communications Letters*, vol. 6, pp. 514–517, Aug 2017.
- [6] B. V. D. Bergh, A. Chiumento, and S. Pollin, "LTE in the sky: trading off propagation benefits with interference costs for aerial nodes," *IEEE Communications Magazine*, vol. 54, pp. 44–50, May 2016.
- [7] M. Mozaffari, W. Saad, M. Bennis, and M. Debbah, "Unmanned aerial vehicle with underlaid device-to-device communications: Performance and tradeoffs," *IEEE Transactions on Wireless Communications*, vol. 15, pp. 3949–3963, June 2016.
- [8] M. M. Azari, F. Rosas, A. Chiumento, and S. Pollin, "Coexistence of terrestrial and aerial users in cellular networks," in *2017 IEEE Globecom Workshops (GC Wkshps)*, pp. 1–6, Dec 2017.
- [9] H. C. Nguyen, R. Amorim, J. Wigard, I. Z. Kovács, T. B. Sørensen, and P. E. Mogensen, "How to ensure reliable connectivity for aerial vehicles over cellular networks," *IEEE Access*, vol. 6, pp. 12304–12317, 2018.
- [10] E. Yanmaz, R. Kuschnig, and C. Bettstetter, "Achieving air-ground communications in 802.11 networks with three-dimensional aerial mobility," in *2013 Proceedings IEEE INFOCOM*, pp. 120–124, April 2013.
- [11] I. Z. Kovács, R. Amorim, H. C. Nguyen, J. Wigard, and P. Mogensen, "Interference analysis for UAV connectivity over LTE using aerial radio measurements," in *2017 IEEE 86th Vehicular Technology Conference (VTC-Fall)*, pp. 1–6, Sept 2017.
- [12] H. C. Nguyen, R. Amorim, J. Wigard, I. Z. Kovács, and P. Mogensen, "Using LTE networks for UAV command and control link: A rural-area coverage analysis," in *2017 IEEE 86th Vehicular Technology Conference (VTC-Fall)*, pp. 1–6, Sept 2017.
- [13] "Evolved universal terrestrial radio access (E-UTRA) physical layer measurements," Tech. Rep. TS 136 214, ETSI, 2011.